

In Silico Screening for Potent Inhibitors against the NS3/4A Protease of Hepatitis C Virus

Arthitaya Meeprasert¹, Thanyada Rungrotmongkol², Mai Suan Li^{3,4,*} and Supot Hannongbua^{1,*}

¹Computational Chemistry Unit Cell, Department of Chemistry, Faculty of Science, Chulalongkorn University, 254 Phayathai Road, Pathumwan, Bangkok 10330, Thailand; ²Department of Biochemistry, Faculty of Science, Chulalongkorn University, 254 Phayathai Road, Bangkok 10330, Thailand; ³Institute of Physics, Polish Academy of Sciences, Al. Lotników 32/46, 02-668 Warsaw, Poland;

⁴Institute for Computational Science and Technology, Quang Trung Software City, Tan Chanh Hiep Ward, District 12, Ho Chi Minh City, Vietnam

Abstract: Hepatitis C virus (HCV) infections are a serious viral health problem globally, causing liver cirrhosis and inflammation that can develop to hepatocellular carcinoma and death. Since the HCV NS3/4A protease complex cleaves the scissile peptide bond in the viral encoded polypeptide to release the non-structural proteins during the viral replication process, this protease is then an important target for drug design. The computer-aided drug design and screening targeted at NS3/4A protease of HCV were reviewed. In addition, using steered molecular dynamics simulations, potent inhibitors of the NS3/4A complex were searched for by screening the ZINC database based upon the hypothesis that a high rupture force indicates a high binding efficiency. Nine top-hit compounds (**59500093, 59784724, 13527817, 26660256, 29482733, 25977181, 28005928, 13527826** and **13527826**) were found that had the same or a greater maximum rupture force (and so assumed binding strength and inhibitory potency) than the four current drugs and so are potential candidates as anti-HCV chemotherapeutic agents. In addition, van der Waals interactions were found to be the main contribution in stabilizing the ligand-NS3/4A complex.

Keywords: NS3/4A protease, hepatitis C virus, steered molecular dynamics simulations.

INTRODUCTION

Hepatitis C viruses (HCV) are enveloped positive single stranded RNA viruses in the *Flaviviridae* family, and are comprised of some eleven main genotypes (30-35% sequence difference between genotypes), multiple subtypes and some 100 strains that show different global distribution/infection patterns. Genotypes 1-3 tend to have a worldwide distribution with genotype 1a accounting for ~60% of the global infections, whilst genotypes 2 and 3 account for around 35% of global infections [1-4]. Genotypes 4-11 are distributed more locally and typically account for a much lower proportion of infections, but local HCV populations and infection patterns can vary considerably from the above global average pattern. This is relevant since the virulence and optimal treatment can vary with each HCV genotype.

Infection with HCV causes liver inflammation that can develop into cirrhosis, hepatocellular carcinoma and death, making hepatitis C one of the public health problems [5, 6]. Moreover, the global number of people infected with HCV is continuously increasing by about 3-4 million each year. The current drug applications used for the treatment of infections are principally the long term (24-48 weeks) administration of (i) peg-interferon (PEG-IFN), (ii) PEG-IFN in combination with ribavirin, and (iii) PEG-IFN/ribavirin with either boceprevir (Victrelis®) or telaprevir (Incivek®), but these exhibit increasing sustained undesirable side effects, such as flu-like symptom, anemia and hemolysis [7, 8]. Moreover, for the common and virulent HCV genotype 1, PEG-IFN combined with ribavirin has an approximate success rate of only 40-50% of treated patients [9-11], compared to almost complete success in the treatment of infection with HCV genotypes 2 and 3. Therefore, HCV inhibitors with an increased efficiency and decreased side effects are urgently needed.

The HCV genome (~ 9,600 nucleotides) is initially translated as a precursor polyprotein (Fig. 1A) and then subsequently processed

by host peptidases and viral proteases on the endoplasmic reticulum (ER) membrane into the four structural proteins (C, E1, E2 and p7) and six non-structural proteins (NS2, NS3, NS4A, NS4B, NS5A and NS5B), which are essential for viral replication cycle.

HCV generally has two principal drug-targets: its RNA polymerase and the protease enzymes. The RNA-dependent RNA-polymerase (RdRp) of HCV, catalyzing the RNA replication, lacks a proofreading activity which results in a high mutation rate and a large number of mutations [12]. The NS3/4A protease plays a critical role in producing the important components for viral RNA replication by cleaving the scissile peptide bond between the junctions of NS3/NS4A, NS4A/NS4B, NS4B/NS5A and NS5A/NS5B. NS3/4A is a serine protease belonging to trypsin/chymotrypsin superfamily, where the H57, D81 and S139 residues form an essential catalytic triad involved in the recognition of the D/EXXXC/T-S/A sequence of substrates [13, 14]. Based on the available structure of HCV protease [15-17], there are three possible sites used for drug design: (i) substrate binding pocket, (ii) NS4A binding groove and (iii) zinc binding site. At the last site, zinc ion is linked to three cysteine residues and a histidine via a water molecule which forms the tetrahedral coordination geometry resulting to non-dominantly specific pocket to any compounds. Since NS4A cofactor binds tightly to NS3 protease, it is rather difficult to develop the suitable inhibitors at the protein-protein binding site [18]. This is thus the substrate binding site only has potential to serve as target for anti-HCV drug design. Since the binding pocket of HCV NS3/4A is likely solvent exposable, shallow and hydrophobic than that of the other proteases such as thrombin and elastase [19], the design and development of drugs that can act as inhibitors of this protease is more challenging. The design of most of the existing protease inhibitors have been designed based on the decapeptide (P6-P4') substrate of NS3/4A by subsequent modification of the functional group to prevent its cleavage by the catalytic residues (reversible competitive inhibitors). Since in other serine proteases the N-terminal products appear to be inhibitors of the enzyme itself including HCV protease (Table 1), then these cleaved products of NS3/4A have also been used to optimize peptidomimetic inhibitors using aldehyde, boronate and α -ketoamide groups [20-24]. For example, the two current drugs, boceprevir and telaprevir (Fig. 2),

*Address correspondence to this author at the Computational Chemistry Unit Cell, Department of Chemistry, Faculty of Science, Chulalongkorn University, 254 Phayathai Road, Pathumwan, Bangkok 10330, Thailand; Tel: +662-218-7602; Fax: +662-218-7603; E-mails: masli@ifpan.edu.pl; supot.h@chula.ac.th

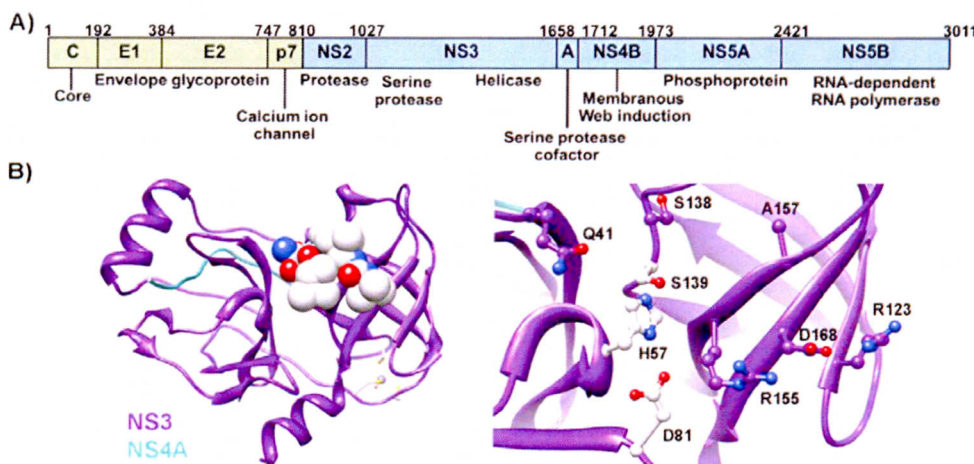


Fig. (1). (A) Polyprotein of hepatitis C virus (HCV), where the green and blue present structural and non-structural proteins, respectively. (B) (Left) Structure of the NS3/NS4A in complex with the inhibitor bound (vdW sphere), and (right) the catalytic triad residues (H57, D81 and S139 in white ball and sticks) and the other residues (violet ball and sticks) at the binding site. (The color version of the figure is available in the electronic copy of the article).

Table 1. The biological activities of NS3/4A substrates and their cleaved products.

Substrate/Cleaved product	K_m (μM) ^a	K_i (μM) ^a
NS3-NS4A		
DLEVVT-STWV	nd ^b	> 500.0
DLEVVT-OH		
NS4A-NS4B		
DEMEEC-ASHLPYK-NH ₂	10.0	0.6
DEMEEC-OH		80.0
DEMEEC-NH ₂		> 500.0
ASHLPYIEQQ-NH ₂		
NS4B-NS5A		
DCSTPC-SGSW-NH ₂	> 1000.0	180.0
DCSTPC-OH		> 300.0
SGSWLRDVWDKK-NH ₂		
NS5A-NS5B		
EDVVAbuC-SMSY-NH ₂	3.8	1.4
EDVVAbuC-OH		> 300.0
SMSYTWTGALKK-NH ₂		

^and, not determined

^b K_m and K_i are taken from the reference [22]

that contain an α -ketoamide instead of a scissile peptide bond, have been used to inhibit the NS3/4A protease by forming a covalent bond to the hydroxyl group of the S139 residue in a reversible manner [23].

The NS3 protein is composed of a serine protease domain at the N-terminal and a helicase/NTPase domain at the C-terminal and forms a non-covalent complex with the NS4A cofactor (Fig. 1B). Among 631 residues of NS3 protein, the minimum residues required for the protease activity is 180 amino acids counting from the N-terminus and 14 amino acids of the NS4A protein which is embedded in the NS3 protease domain for activating the protease enzyme function. The NS3 protease has two sub-domains, N-

terminus (residues 1-93) and C-terminus (residues 94-180), where each sub-domain contains the conventional six-stranded β barrel [6, 13, 25]. Even though the reported full-length NS3/4A crystal structure [26] and molecular dynamics study [27] showed that the NS3/4A active site is located near helicase-protease interface resulting to the formation of ligand-helicase interactions, the kinetic properties of truncated protease is likely similar to those of the full-length NS3/4A. Thereby, several previous studies on the HCV NS3/4A protease were focused on the truncated protease [28-31]. In the crystal structure of NS3 protease without NS4A cofactor binding [32, 33], the imidazole ring of H57 catalytic residue is moved out from the S139 reaction center residue and thus it is unable to

abstract the proton from the hydroxyl group of S139 while the carboxylic group of D81 turns away into the direction that cannot stabilize the H57. Therefore, the presence of NS4A cofactor is needed to adjust the three catalytic residues of NS3 protease into the active conformation suitable for deprotonation of S139 and Michaelis addition.

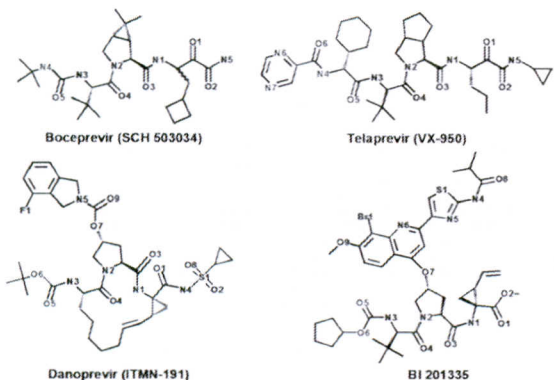


Fig. (2). Chemical structures of the four NS3/4A protease inhibitors: boceprevir, telaprevir, danoprevir (ITMN-191) and BI201335.

In addition, two non-covalent inhibitors with strong electrostatic interactions with the NS3/4A catalytic pocket have also been developed (BI201335 and danoprevir (ITMN-191); Fig. 2) and are currently in phase 3 and phase 2 clinical trials, respectively [34]. Danoprevir (0.2 nM) showed an approximately 400-fold higher efficiency compared to boceprevir (80 nM) and telaprevir (87 nM) in the treatment of HCV genotype 1 infections in preclinical trials [35]. BI201335 (1.2 nM) inhibited the NS3/4A protease with a similar potency to boceprevir (1.1 nM), but was about three-fold more effective than telaprevir (3.2 nM). Moreover, whilst BI201335 showed a high capability to inhibit the NS3/4A activity of HCV genotypes 1, 4, 5 and 6, it was less potent against genotypes 2 and 3 being about 50-fold and 190-fold lower than against genotype 1 [36]. A subnanomolar inhibition activity of danoprevir was similarly found against these four genotypes, however its potency was decreased about 10-fold for inhibiting genotypes 2 and 3 [35]. Additionally, the side effects are commonly detected after treatment with boceprevir or PEG-IFN plus ribavirin [37]. The combination of these three drugs affect more serious anemia. Moreover, drug

resistance has already been reported for the currently available commercial anti-HCV drugs, as summarized in Table 2, and is increasing in frequency.

Recently, various computational techniques are available and potentially useful for designing, developing and exploring the novel inhibitors with higher efficiency and specificity than the existing drugs as well as understanding the key drug-target interactions in a variety of diseases such as influenza [43-45], human immunodeficiency virus (HIV) infection [46], tuberculosis [47], chikungunya [48] and cancer [49]. The current available tools are for example molecular docking, quantitative structure-activity relationship (QSAR), comparative molecular field analysis (CoMFA), comparative molecular indices analysis (CoMSIA), molecular dynamics (MD) simulation and etc.

da Cunha and co-workers [50] employed CoMFA approach to determine the best 3D-QSAR model on BILN 2061 derivatives. They predicted that substitution of the carbamate group of BILN 2061 with bulky group leaded to an increase in the inhibition efficiency, whereas the bulky group at the thiazole ring provided the unfavorable interaction. The potency of inhibitor can also be enhanced by replacing the thiazole ring with the low electron density functional group. It is well-known that the functional side chain of P2 and P3 residues of peptide inhibitors favors to be hydrophobic and hydrophilic groups, respectively. The 3D-QSAR contour maps of tetrapeptide analogue inhibitors [51] presented that the large favored negative charge contour of P3 residue apparently oriented toward the positively charged side chain of K136 while the favored hydrophobic contour allowed the P3 side chain to preferentially occupy in the hydrophobic pocket formed by the V132, V158 and C159. In addition, the pharmacophore results suggested that the modification on P3 residue by extending its side-chain length could expand the binding interaction with the S3 subsite. From the observed success of these ketoamide substituted compounds in inhibiting the HCV NS3/4A, derivatives have been continuously developed so as to try to obtain a higher inhibition efficacy [52-55]. For example, narlaprevir, a second generation NS3/4A inhibitor, was designed based on the boceprevir structure and gave about a 10-fold improved inhibition [52]. The CoMFA, CoMSIA and HQSAR techniques were applied to build a QSAR model to investigate the relationship between the structure of the inhibitor and its biological activity, an advantage if not prerequisite for the design and development of higher efficiency inhibitors, using the 190 derivatives of narlaprevir as the initial source for screening [31, 56-62]. The CoMFA contour map (Fig. 3) suggested that the R1 and R2 groups of narlaprevir should be modified with a larger chain, such as cyclic rings. A negatively charged R1 group (sulfonamide group for example) and positively charged R4 group were predicted to increase

Table 2. Drug resistance profile of the four currently available NS3 protease HCV inhibitors

Residue	Mutation	Inhibitors
V36 [2, 38-41]	A, M, G	Boceprevir, Telaprevir
Q41 [40]	R	Boceprevir, Danoprevir
F43 [40]	S, C	Boceprevir, Telaprevir, Danoprevir
T54 [2, 38-42]	A, S	Boceprevir, Telaprevir, BI201335
R155 [2, 38-40, 42]	K, T, Q	Boceprevir, Telaprevir, BI201335, Danoprevir
A156 [2, 38-40, 42]	S, T, V	Boceprevir, Telaprevir, BI201335, Danoprevir
D168 [2, 42]	A, V, G	BI201335, Danoprevir
V170 [2, 40]	A	Boceprevir, Telaprevir

the inhibition efficiency. Notice that the activity becomes worse if the R4 group is a large side chain and so this side chain should be small. Among the 16 best designed compounds, the 4 compounds had the highest predicted binding affinities that might be the anti-HCV drug candidates.

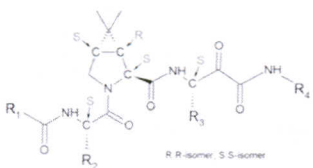


Fig. (3). The structure of the narlaprevir derivative scaffold [31] (© 2012 Bentham Science Publishers Ltd.).

The molecular docking approach is generally employed for virtual screening and predicting the binding pattern in an active site of bimolecular systems, since it computationally uses up less CPU time. However, if the movement of the receptor is regulated as a rigid molecule, the prediction ability of molecular docking is rather limited and sometimes inaccurate [63, 64]. For example, a range of indole derivatives were designed as NS3/4A inhibitors and docked into the NS3/4A binding site using molecular docking but subsequently some of the docking results were found to be in contrast to the observed experimental inhibition activity [65]. Besides the standard molecular docking (flexible ligand docking) method, the flexible receptor docking or induced-fit docking (GENIUS) approach allows the conformational change of both the ligand and receptor [66]. This method was used on the NS3/4A protease of HCV to screen for novel inhibitors. Initially 97 compounds were screened out of 166,206 compounds using the ranked GENEIUS scores, but only 27 of these 97 compounds were experimentally found to show more than 50% inhibition at 100 μ M. The two common scaffolds from these 27 compounds were then used for a 2D-similarity search. Among the 140 matching compounds found the five compounds that was a new class of anti-NS3/4A candidate scaffold with IC₅₀ values of < 10 μ M. This finding may useful for the further drug design and development. The higher accuracy approaches, such as molecular mechanics Poisson-Boltzmann surface area (MM-PBSA), molecular mechanics generalized Born surface area (MM-GBSA), linear interaction energy (LIE), thermodynamic integration, potential mean force (PMF) and so on, are widely used and provide more reliable results, but they require a significantly higher computational time that restricts their application to screening larger datasets. As in previous work [67], molecular docking, MD simulation and MM-PBSA methods were used in order to investigate the binding interaction between NS3/4A and polyphenol derivatives. Since the crystal structures of these complexes were not available, molecular docking was subsequently used to dock each compound into the substrate binding site (H57, D81, G137, S139, A156 and A157). The MM-PBSA result gave the correlation coefficient between predicted and experimental binding free energies of 0.96. Ideally, a trustworthy method that demands a relatively low CPU time is optimal for high throughput screenings that are otherwise logically impractical with the CPU intensive methods. The steered molecular dynamics (SMD) approach has been proposed as one such potential good choice as it can be rapidly used to investigate the unbinding process of ligands from the receptor, the unfolding mechanism of bimolecular systems, transportation of small molecules through channels and for screening hit-lead compounds [68-71]. In the last case, it is based on the hypothesis that the larger rupture force is required to pull a higher susceptibility ligand out from its receptor. Recently, the SMD approach was successfully applied to evaluate the binding affinity of the neuraminidase inhibitors of influenza A pH1N1 virus as well as other designed compounds obtained from the NCIDS library [70].

This work then focuses on screening for potential inhibitors of the HCV NS3/4A protease complex. To this end the search for ligands that are potential new potent anti-HCV drug candidates was performed by screening the ZINC database [37] using SMD simulations to remove each docked ligand from the NS3/4A (HCV genotype 1a) binding pocket with a constant velocity. Afterwards, the binding efficiency of each ligand was predicted from the maximum pulling force (F_{max}). Note that the four known HCV NS3/4A protease inhibitors (boceprevir, telaprevir, BI201335 and danoprevir) were also included in this SMD screen for validation by comparison of the obtained theoretical data to their known experimental inhibition activities [35, 36].

MATERIALS AND METHODS

NS3/4A Protease and Inhibitor Complexes Preparation

The three-dimensional structures for the complexes of NS3/4A protease of HCV genotype 1a bound with boceprevir, telaprevir and danoprevir were obtained from the Protein Data Bank (PDB) with PDB entry codes 2OC8 [72], 2P59 [73] and 3M5L [17], respectively. In contrast, the BI201335 complex was modeled from the X-ray structure of this compound bound to the HCV genotype 1b protease (3P8N [16]) by employing the macromolecules tool in the Discovery Studio 2.5^{Accelrys Inc}. The protonation state of all ionizable amino acids (R, K, D, E and H) were considered at pH = 7.0. Additionally, the H protonation state was determined by considering the possibility of hydrogen bond formation with the surrounding residues. The development of atomic charges and empirical force field parameters for the inhibitor were developed according to the standard procedure [49, 74-76]. The atomic charges of each drug were calculated using the HF/6-31g(d) method with the Gaussian03 software [77], which were then fitted into RESP charges using the ANTECHAMBER module implemented in AMBER10 [78, 79]. The atom types and the other parameters of each ligand were assigned by AMBER force fields [80] and GAFF [81]. Afterwards, the ACPPYPE [82] was used to convert the AMBER file format to GROMACS format.

Set of Ligands and Molecular Docking

To search for potent inhibitors of the NS3/4A protease of HCV genotype 1a, the ZINC database [83] (over 21 million compounds in ready-to-dock 3D formats) was first selected to collect 40 compounds using the criteria that the ligand-target is a serine protease enzyme and the net charge of the ligand is less than or equal to 1. Atomic charges, atom types and other parameters of all ligands were prepared as described above. Subsequently, each ligand was then flexibly docked into the rigid NS3/4A binding pocket using the GOLD (Genetic Optimization for Ligand Docking) suite version 5.1 from the Cambridge Crystallographic Data Center (CCDC). The Genetic Algorithm (GA) was applied to explore the possible conformations and orientations of all compounds in the drug binding site where CHEMPLP was used as the fitness function [84]. For each docking simulation, 30 GA runs were performed with 100,000 genetic operations and a population size of 100 chromosomes. Note that the docked results with 30 GA runs are relatively similar to the higher GA runs up to 50 and 100. The crossover, mutation and migration frequencies were set at 95, 95 and 10, respectively, while the selection pressure was fixed at 1.1. However, the GA will be terminated early if the top three dockings are within 0.15 nm of the RMSD of all atoms. With respect to the flexibility of the ligand, the protonated carboxylic acids and all planar moieties containing R-NR₁R₂ were allowed to flip. The 1.2 nm sphere radius around the catalytic residue S139 was defined as a binding site. The conformer with the highest CHEMPLP docking score and intensively interacting with the NS3/4A binding residues was considered as the best binding mode and adopted as the starting structure for SMD simulations in the next step. Again, the partial charges and parameters for

each compound from the ZINC database were prepared in the same way as the known inhibitors (described above).

SMD Simulations

The NS3/4A protease-ligand complexes were embedded in a rectangular box of dimensions of $7.0 \times 7.5 \times 10.0$ nm that contained ~16,000 molecules of TIP3P water [85]. Chloride ions were added to neutralize the whole system. The center of mass of the NS3/4A protease was placed at 3.50, 3.75 and 3.50 nm. The unbinding tunnel's vector starting from the protein active site to the calculated end point of tunnel was relocated and re-rotated to Z-direction using editconf module implemented in GROMACS. Note that the vector direction was checked by adding dummy atoms to identify its direction prior to SMD performed. All molecular dynamics (MD) and SMD simulations were performed using the GROMACS 4.5.5 package [86, 87] with the AMBER ff03 force field [80]. Firstly, the added solvent and ions were energetically minimized using steepest descent (SD) while the other molecules were constrained. The receptor was then minimized by SD method with a constrained solvent. Finally, the entire system was minimized by SD and conjugated gradient (CG), respectively. Each minimization converged when the maximum force was ≤ 100 kJ/mol·nm. MD simulations were initially heated from 0 to 298 K for 100 ps with the *NVT* ensemble using the Berendsen procedure. Afterwards, the simulations with the *NPT* ensemble were performed at 298 K and a pressure of 1 atm (~101.33 kPa) for 200 ps using the Parrinello-Rahman pressure coupling approach to maintain a constant pressure, whilst the solute was restrained with 200 kJ/mol·nm². Thereafter, the restrained force was decreased to 100 kJ/mol·nm², and the simulation was continuously equilibrated for 200 ps. To ensure that the complex structure was stable prior to SMD calculation, the system was then fully equilibrated for 1000 ps. The LINC algorithm was applied to constrain all bonds [88]. A time step of 2 fs with a van der Waals interaction cut off of 1.4 nm was used. Meanwhile, the long-range electrostatic interactions were evaluated by means of the particle mesh Ewald (PME) summation method [89, 90]. The non-bonded interaction pair-list was truncated at 1.0 nm and updated every 10 fs.

After equilibration, the bound ligand was pulled out from the binding pocket of the NS3/4A protease with a constant velocity (v) of 0.005 nm/ps along the z-direction using harmonic potential on the ligand, whereas the C-alpha atoms of all amino acids were restrained. The force was applied on an atom close to the center of mass of the ligand with a spring constant (k) of 600 kJ/mol·nm² (~996 pN/nm). While a pulled ligand was moving, the hydrogen bonds with NS3/4A were gradually ruptured. The total force can be measured via $F = k(vt - x)$, where x is the displacement of pulled atom from the starting position. Four and three independent simulations were performed for each known inhibitor and ZINC compound, respectively, using the different seed numbers in order to confirm the consistency of results.

RESULTS AND DISCUSSION

Choice of Pulling Path

Caver 2.1 [91, 92], implemented in Pymol, was employed to generate the possible pathways of pulling a ligand out from the drug binding site of the NS3/4A protease. As well-known that the rupture force is sensitive to the pulling direction [93, 94], therefore it is needed to verify which pathway is most suitable for ligand unbinding. The three possible pathways for unbinding ligands from the NS3/4A active site together with their average radius and depth are shown in (Fig. 4A). Since the easiest or main unbinding pathway could confer the lowest rupture force, it is hypothesized that the shallowest and/or widest tunnel could be the easiest pathway. This is because the leaving ligand supposes to interact with minimal number of amino acids along the tunnel. According to this hypothesis, the pathway 1 with an average radius of 0.13 nm and depth of 1.40 nm was chosen. Additionally, the seven possible pathways of

pulling were generated (pathways 4-10 in (Fig. S1) of the supporting information) in order to assure that the pathway 1 is the main tunnel. Even though the tunnels 4 (0.17 nm), 9 (0.14 nm) and 10 (0.17 nm) seem rather wider in comparison with that of the tunnel 1 (0.13 nm), their lengths are significantly longer by approximately 0.81, 0.01 and 2.64 nm, respectively. Whereas, the rest tunnels (pathways 5-8) are slightly either narrower or deeper than those of pathway 1.

To ensure that the first tunnel had the smallest rupture force for pulling the ligand, boceprevir was pulled out from the pathways 1-3. The derived force-time and force-displacement profiles are summarized in (Fig. 4B and 4C) where the displacement (extension) refers to the distance between the ligand positions at time $t = t_x$ and $t = t_0$. The rupture force (F_{max}) obtained from the third tunnel was much higher than that in the other two tunnels, since its cavity (Fig. 4A) is rather narrow at the active site as well as significantly longer (3.52 nm). Interestingly, among pathways 1-3, the direction of the third tunnel is only pointed to HCV helicase domain [26, 27] leading to deeper tunnel which could consequently result in a higher rupture force. Meanwhile the average radius in pathway 2 was the smallest in width (0.09 nm) but the F_{max} of the first pathway displayed a slightly lower F_{max} than the second tunnel in accordance with its 0.89 nm shorter length. In addition, the first two pathways reached the maximum point at almost the same time (~226 ps), while the third pathway took ~ 50 ps longer (Fig. 4B and 4C). After that the interaction between the NS3/4A and boceprevir suddenly decreased together in all three cases to an elongation of the extended distance (ligand displacement) of more than ~ 1.5 nm (Fig. 4C).

Taken together, the first tunnel, which is surrounded by the V55, H57, S139, G140, F154, R155 and A156 residues of the NS3/4A complex, was the easiest way for the ligand to escape from the NS3/4A binding site to the bulk phase. Accordingly, this was used in further simulations for screening the compounds by SMD simulations.

Validity of the SMD Approach

To test the potential reliability of the SMD simulations prior to using this approach to screen for hit-lead compounds for the NS3/4A protease inhibition from the ZINC database, the four known NS3/4A protease inhibitors (boceprevir, telaprevir, BI201335 and danoprevir) were pulled out from the binding pocket along pathway 1 (Fig. 4). Their geometries at the equilibrium state were then superimposed, as shown in (Fig. S3). The force-time and force-displacement profiles of each of the four inhibitors are plotted in (Fig. 5), while the profiles obtained from the other three SMD simulations with different starting velocities are given in (Fig. S1) (supporting information). With respect to the force-time profile (Fig. 5A), the force increased linearly over time to reach the maximum force, defined as the rupture force (F_{max}), due to the gradual disruption of the hydrogen bonds, electrostatic and van der Waals interactions enforced by the increased distance between the ligand and binding site induced by the external applied force at a constant velocity of 0.005 nm/ps. After reaching F_{max} the force immediately decreased, although a minor peak was possibly observed due to the newly formed interactions with the residues located along the pathway, as seen for BI201335 for example.

With respect to the force-displacement plot (Fig. 5B), the boceprevir, telaprevir and BI201335 ligands successfully escaped from the NS3/4A protease at nearly the same distance as each other at ~1.5 nm and after ~350 ps (Fig. 5A), whilst the danoprevir was freed later (~400 ps) at a distance of ~2.0 nm. That the NS3/4A-danoprevir complex takes the longest time and the highest force to remove it suggests that it is the most stable complex, whilst according the NS3/4A-telaprevir would be the worst due to the required lowest applied force to unbind it. The susceptibility of boceprevir

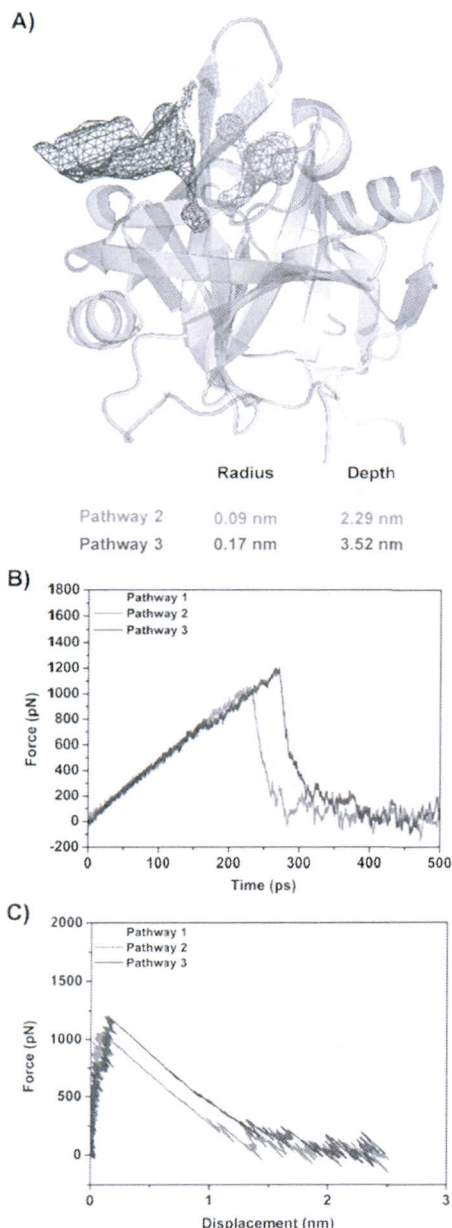


Fig. (4). (A) Three possible pathways shown with their average radius and depth for ligand unbinding path constructed by pulling boceprevir from the NS3/4A binding site. (B) The force-time and (C) force-displacement profiles of boceprevir along the three pathways shown in (A).

towards the NS3/4A protease was predicted to be comparable to that of BI201335. For comparison with the experimentally derived data [22, 23], the theoretically (SMD) derived rupture force (F_{\max}) obtained from Fig. 5 was plotted with the experimental binding free energies, derived from their reported inhibition activities as IC_{50} [35] and K_i [36] values (Fig. 6). The F_{\max} values obtained from the SMD simulations corresponded relatively well to the experi-

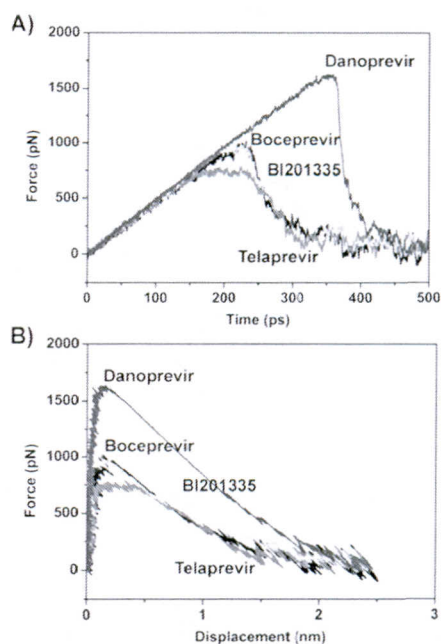


Fig. (5). (A) The force-time and (B) the force-displacement profiles of the four inhibitors pulled from the NS3/4A protease binding site through the selected tunnel (pathway 1 in Fig. 4A), where in (A) the x-axis refers to the extended distance from the reference position of the ligand (at $t = 0$).

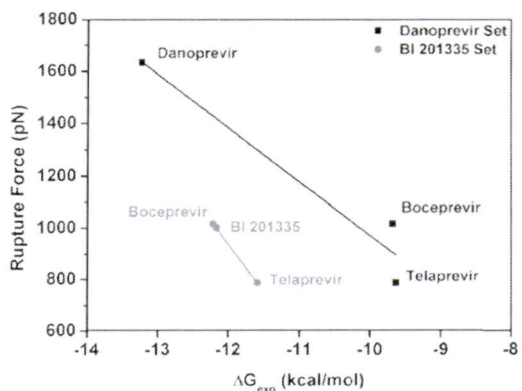


Fig. (6). The correlation between the rupture force (F_{\max}) and the calculated binding free energies obtained from the experimental values, based on $\Delta G_{\exp} = RT \ln(K_i / IC_{50})$, where $R = 1.987 \times 10^{-3}$ kcal/mol, $T = 298$ K, K_i is inhibition constant and IC_{50} is the half maximal inhibitory concentration.

mentally derived data, with the binding efficiency ranked (highest to lowest) as danoprevir > boceprevir ~ BI201335 > telaprevir. Therefore, the SMD approach was viewed as having the potential to obtain qualitatively reliable binding affinities and so could be used for screening the hit-lead compounds of the NS3/4A protease of HCV from the ZINC database.

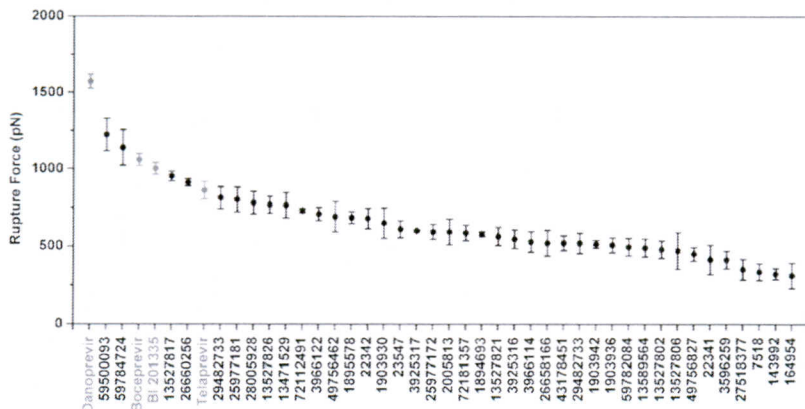


Fig. (7). Ranking of the binding affinity to the NS3/4A protease of the top 40 ligands from the ZINC database and the four currently used HCV inhibitors (shown in grey) for comparison.

Ranking of Binding Affinity of Ligands

After three independent MD simulations for each ligand-NS3/4A protease complex, each compound from the ZINC database was pulled out from the NS3/4A binding pocket using the same procedure applied for the known inhibitor-protease complex described above. The average F_{\max} values derived from the multi-simulations with their standard deviations for all 40 compounds were ranked with those of the four inhibitors in Table S1 (supporting information) and plotted in (Fig. 7). The CHEMPLP scores derived from the docking analysis are also given in Table S1 for comparison.

In comparison between docking score and SMD rupture force for the 44 ligands (Table S1), although the best potent ligand predicted from both methods is danoprevir, the docking cannot well predict the binding affinity of the known inhibitors (danoprevir > BI201335 >> telaprevir > boceprevir) unlike the SMD (danoprevir > boceprevir ~ BI201335 > telaprevir). This is because the docking method contains the uncontrollable factors such as neglecting the protein dynamics and limiting in the trial number of ligand position. Additionally, the CHEMPLP scoring function is a force field based scoring which ignores the internal protein energy [95]. Therefore, the top 10 ligands screened from the calculated rupture force are further discussed in details.

From the F_{\max} values, danoprevir, which is currently in phase 2 clinical trials, was predicted to have the highest efficiency of ligand binding against the NS3/4A protease of HCV (genotype 1a) with an F_{\max} value of approximately 1572 pN. The ZINC compounds **59500093** and **59784724** (F_{\max} values of 1222 and 1137 pN, respectively) were predicted to interact with the NS3/4A protease considerably better than the two approved drugs of boceprevir and telaprevir (F_{\max} values of 1058 and 859 pN, respectively) and better than BI201335 (1000 pN) that is currently in phase 3 clinical trials. In addition, compounds **13527817** (951 pN) and **26660256** (912 pN) are predicted to form a more stable complex with NS3/4A than telaprevir. However, there were an additional five ligands (**29482733**, **25977181**, **28005928**, **13527826** and **13471529**; at 811, 800, 780, 767 and 763 pN, respectively) that were capable of binding to the NS3/4A protease within the range of one standard deviation of that for telaprevir (859 ± 58 pN). Apart from these nine compounds, the remaining 31 ligands form the top 40 hits obtained from screening the ZINC database showed lower F_{\max} values (< 750 pN) that were less than the one standard deviation limit of telaprevir (800 pN) and so are likely to be inferior inhibitors. Accord-

ingly, these nine best (highest F_{\max}) compounds from the ZINC database (**59500093**, **59784724**, **13527817**, **26660256**, **29482733**, **25977181**, **28005928**, **13527826** and **13527826**) were selected as potential candidates for the NS3/4A inhibitors of HCV genotype 1. Their force-time and force-displacement profiles are summarized in (Fig. 8). It can be seen that these compounds were placed in the similar orientation as the four known inhibitors (Fig. S3). Interestingly, the four screened compounds (**59500093**, **59784724**, **13527817** and **26660256**) with F_{\max} values that were greater than that for telaprevir all contain an aromatic ring that occupied the S2 binding pocket.

The time dependence of the van der Waals (E_{vdW}) and electrostatic (E_{ele}) interactions between the top ranked 13 ligands and the NS3/4A residues obtained from the first simulation are depicted in (Fig. 10). The number of hydrogen bonds per unit time is plotted in (Fig. 9). It is worth noting that in all the systems except for **59784724**, BI201335 and **29482733**, the vdW interaction is noticeably higher than electrostatic interaction along the pulling time. To understand the ligand-target interactions that potentially correspond to the binding efficiency, the summation of the vdW and electrostatic energies obtained at F_{\max} were considered. Among the 13 ligands, danoprevir, formed six hydrogen bonds with the active site residues, showed the lowest energy summation of -82 kcal/mol (E_{vdW} and E_{ele} of -49 and -33 kcal/mol) at $t \approx 375$ ps and afterwards all the interactions were suddenly lost. The screened **59500093** and **59784724** compounds, which contain macrocyclic and isoindole rings as danoprevir, had a relatively high energy summation (-78 and -72 kcal/mol, at $t \approx 250$ ps). In the case of BI201335, the carboxylate group at the P1 moiety can interact with the G137 and S139 residues at the NS3/4A catalytic pocket leading to a higher net negative value than for the other compounds. At $t \approx 200$ ps, compounds **13527817** and **26660256** provided a kcal/mol higher E_{ele} contribution at F_{\max} than telaprevir, whilst their vdW energies were almost equal. Although the energy summation of the other eight ligands was not significantly lower, they moved out of the NS3/4A binding pocket faster ($t < 200$ ps).

By following the SMD snapshot of NS3/4A-danoprevir complex at the equilibrium state (before pulling the ligand out of pocket), it was presented that the danoprevir was surrounded by Q41, T42, F43, V55, H57, Q80, D81, R123, I132, L135, K136, G137, S138, S139, F154, R155, A156, A157, C159 and D168 (Fig. 11A where the nine selected residues were shown). This inhibitor was strongly stabilized via the hydrogen bonds with H57, K136,

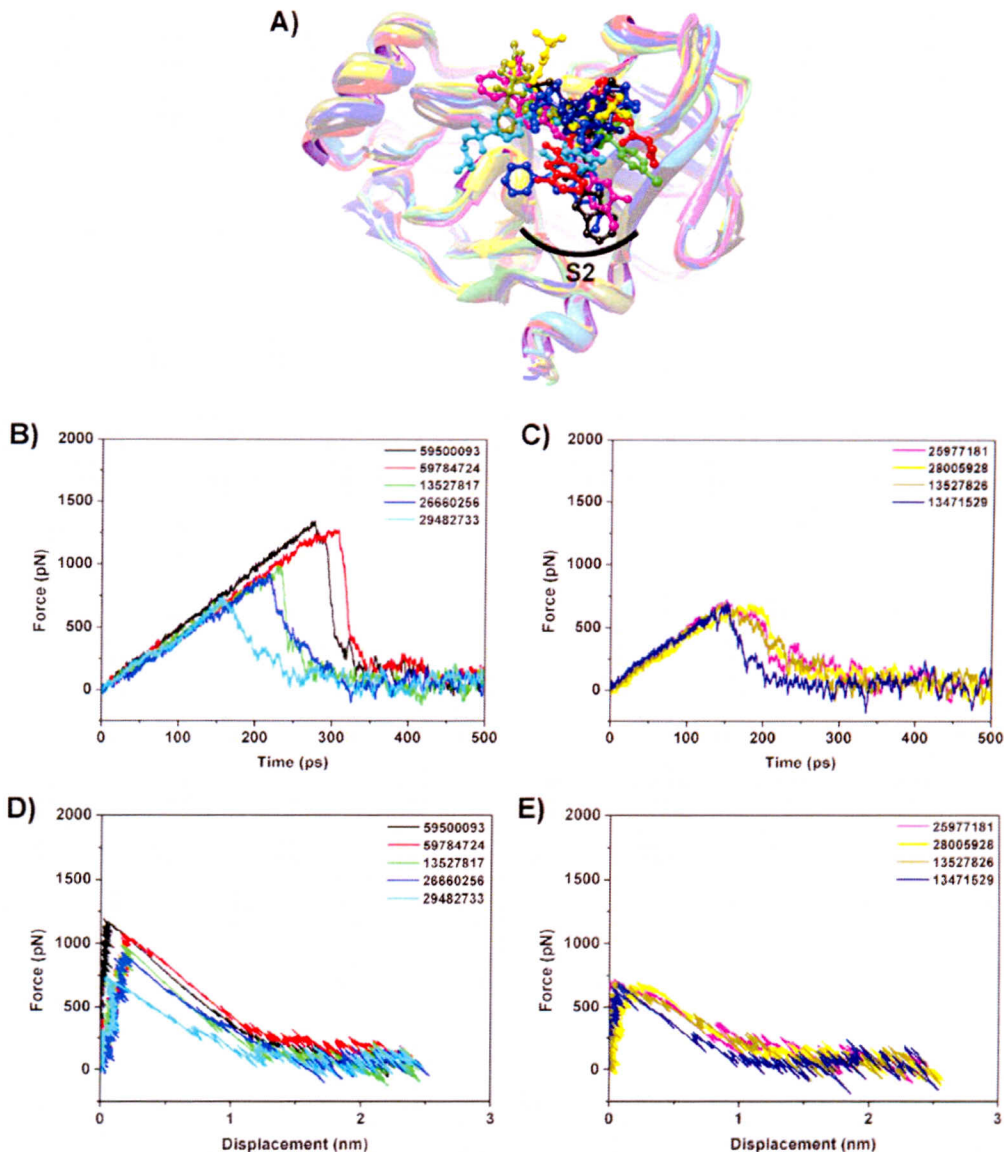


Fig. (8). (A) Superimposition of the last snapshots for NS3/4A in complex with the best nine screened compounds from the ZINC database: 59500093 (black), 59784724 (red), 13527817 (green), 26660256 (blue), 29482733 (cyan), 25977181 (pink), 28005928 (yellow), 13527826 (olive green) and 13471529 (navy blue). The (B) and (C) force-time profiles, and (D) and (E) force-displacement profiles were obtained from the representative trajectories. (The color version of the figure is available in the electronic copy of the article).

G137, S139, R155 and A157 (Fig. 12A). At the maximum peak of pulling force (Fig. 5 at $t = 385$ ps), the sulfone group of danoprevir and the side chain of Q41 were flipped together to form a new hydrogen bonding interaction (with a distance of 0.33 nm in Fig. 12B), while one more water was detected and acted as a center of hydrogen bond network between its carbamate oxygen atom and the two residues, A157 and C159. Meanwhile, the other binding site residues were slightly changed since the center of mass of danoprevir was moved away only about 0.16 nm from the pocket resulting in a loss of interaction with the H57. Likewise, many water mole-

cules gradually came closer to the drug binding site in an effort to solvate, occupy and stabilize the binding pocket instead of a pulled ligand (Fig. 11).

CONCLUSION

The SMD technique was applied to screen for potentially potent anti-HCV agents from the ZINC database based on the hypothesis that a high required rupture force (F_{\max}) for pulling the ligand out of the NS3/4A binding site equates to a high predicted binding affinity and so inhibition efficiency. To validate the method, the four

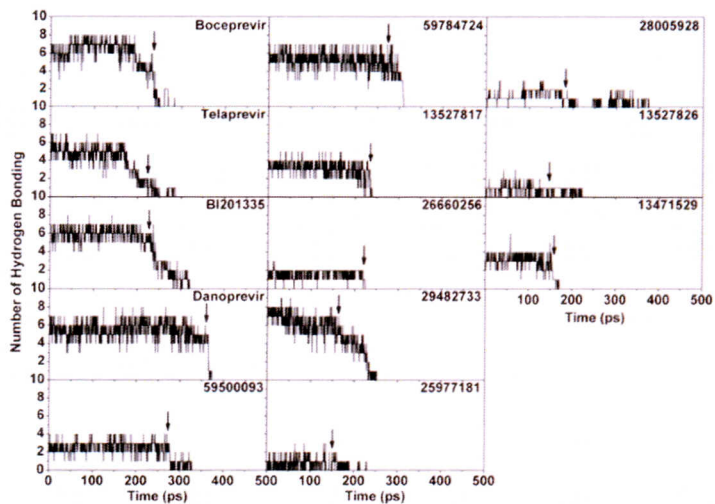


Fig. (9). Time dependencies of the hydrogen binding number of top 13 ligands, the arrow pointed at F_{\max}

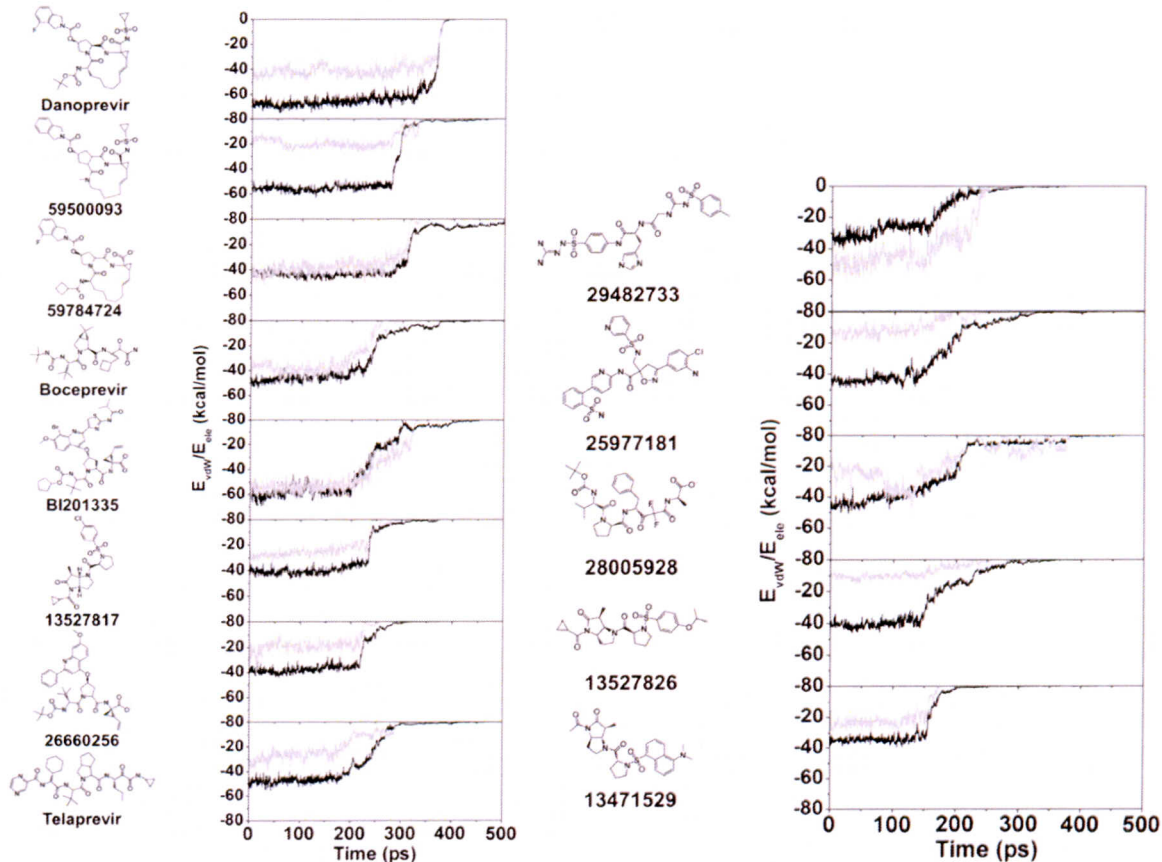


Fig. (10). Electrostatic (E_{ele}) and van der Waals (E_{vdW}) energies (shown in grey and black line, respectively) as the ligand is withdrawn at a constant force per unit time for the top thirteen ligands.

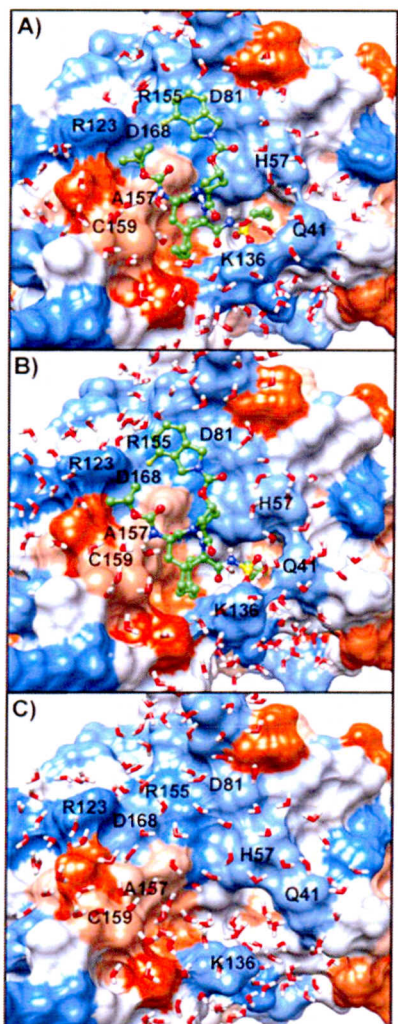


Fig. (11). Close up of the NS3/4A protease in complex with danoprevir (green ball and stick model) at (A) the equilibrium state (before pulling), (B) the maximum point (F_{\max} at $t = 385$ ps in Fig. 4), and (C) the independent state (after passing the maximum point at $t = 450$ ps). The blue and orange colors represent hydrophilic and hydrophobic surfaces, respectively (The color version of the figure is available in the electronic copy of the article).

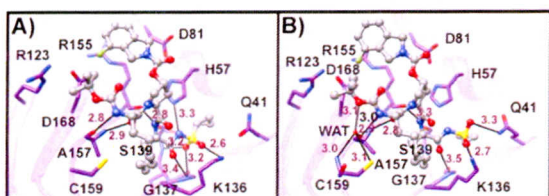


Fig. (12). Hydrogen bond formation between danoprevir and its binding residues in HCV NS3/4A protease at (A) the equilibrium state, (B) the maximum pulling force in correspondence to (Fig. 11) (The color version of the figure is available in the electronic copy of the article).

known HCV inhibitors (boceprevir, telaprevir, danoprevir and BI201335) were also subjected to the same SMD analyses, where the derived F_{\max} values were found to be in good agreement with the experimentally derived inhibition activity data. According to the ranked F_{\max} , the 40 top hit compounds from the ZINC database were reduced to nine (59500093, 59784724 13527817, 26660256, 29482733, 25977181, 28005928, 13527826 and 13471529) that were, from the above assumption, likely to be as good as or better than the four current inhibitors. Compounds 59500093 and 59784724 were predicted to have a higher potential than the existing commercial drugs (boceprevir and telaprevir) and the BI201335 inhibitor that is currently in clinical phase III trials. Compounds 13527817 and 26660256 were suggested to have a better inhibition efficiency than telaprevir (but not boceprevir or BI201335), whereas the remaining five compounds were predicted to be broadly the same as telaprevir. Therefore, these nine top-hit ligands may serve as potential NS3/4A protease inhibitors or be further used as templates for lead optimization. In addition to the predicted binding affinities, derived from the theoretically obtained F_{\max} values, the vdW interaction was found to have a higher contribution towards stabilizing the ligand-NS3/4A interaction than electrostatic interactions.

CONFLICT OF INTEREST

The authors confirm that this article content has no conflicts of interest.

ACKNOWLEDGEMENTS

This work was supported by the Ratchadapiseksomphot Endowment Fund of Chulalongkorn University (RES560530217-HR), and the Higher Education Research Promotion and National Research University Project of Thailand, Office of the Higher Education Commission (HR1155A). The Thai Government Stimulus Package 2 (TKK2555) under the Project for Establishment of Comprehensive Center for Innovative Food, Health Products and Agriculture is greatly acknowledged for computing resources. A.M. thanks the Royal Golden Jubilee Ph.D. Program (PHD/0271/2549) and T.R. thanks the grants for the development of new faculty staff (the Ratchadapiseksomphot Endowment Fund). M.S.L. thanks Narodowe Centrum Nauki in Poland (grant No 2011/01/B/NZ1/01622 and Department of Science and Technology at Ho Chi Minh city, Vietnam for the financial support.

SUPPLEMENTARY MATERIAL

Supplementary material is available on the publishers Web site along with the published article.

ABBREVIATIONS

ACPPYME	=	AnteChamber PYthon Parser interfacE
AMBER	=	Assisted model building with energy refinement
CCDC	=	Cambridge crystallographic data center
CG	=	Conjugated gradient
CoMFA	=	Comparative molecular field analysis
CoMSIA	=	Comparative molecular indices analysis
ER	=	Endoplasmic reticulum
GA	=	Genetic algorithm
GAFF	=	General AMBER force field
GOLD	=	Genetic optimization for ligand docking
GROMACS	=	GROningen MAchine for Chemical Simulations
HCV	=	Hepatitis C virus
HF	=	Hartree-Fock
HIV	=	Human immunodeficiency virus

LIE	=	Linear interaction energy
LINC	=	Linear constraint solver
MD	=	Molecular dynamics
MM-GBSA	=	Molecular mechanics generalized Born surface area
MM-PBSA	=	Molecular mechanics Poisson-Boltzmann surface area
NCIDS	=	NC Office of Indigent Defense Services
PDB	=	protein data bank
PEG-IFN	=	Peg-interferon
PLP	=	Piecewise linear potential
PME	=	Particle mesh Ewald
PMF	=	Potential mean force
QSAR	=	Quantitative structure-activity relationship
RESP	=	Restrained electrostatic Potential
RMSD	=	Root-mean-square deviation
SD	=	Steepest descent
SMD	=	Steered molecular dynamics
vdW	=	Van der Waals
X-ray	=	Crystallographic spectroscopy

REFERENCES

- [1] Chevaliez S, Bouvier-Alias M, Brillet R, Pawlotsky JM. Hepatitis C virus (HCV) genotype 1 subtype identification in new HCV drug development and future clinical practice. *PLoS One* 2009; 4: e8209.
- [2] Rydberg EH, Cellucci A, Bartholomew L, et al. Structural basis for resistance of the genotype 2b hepatitis C virus NS5B polymerase to site a non-nucleoside inhibitors. *J Mol Biol* 2009; 390: 1048-59.
- [3] Simmonds P. Genetic diversity and evolution of hepatitis C virus – 15 years on. *J Gen Virol* 2004; 85: 3173-88.
- [4] Simmonds P, Bukh J, Combet C, et al. Consensus proposals for a unified system of nomenclature of hepatitis C virus genotypes. *Hepatology* 2005; 42: 962-73.
- [5] Bostan N, Mahmood T. An overview about hepatitis C: a devastating virus. *Crit Rev Microbiol* 2010; 36: 91-133.
- [6] Lauer GM, Walker BD. Hepatitis C virus infection. *N Engl J Med* 2001; 345: 41-52.
- [7] Durantel D, Escuret V, Zoulim F. Current and emerging therapeutic approaches to hepatitis C infection. *Expert Rev Anti Infect Ther* 2003; 1: 441-54.
- [8] Ferguson MC. Current therapies for chronic hepatitis C. *Pharmacotherapy* 2010; 31: 92-111.
- [9] Fried MW, Shiffman ML, Reddy KR, et al. Peginterferon alfa-2a plus ribavirin for chronic hepatitis C virus infection. *N Engl J Med* 2002; 347: 975-82.
- [10] Manns MP, McHutchison JG, Gordon SC, et al. Peginterferon alfa-2b plus ribavirin compared with interferon alfa-2b plus ribavirin for initial treatment of chronic hepatitis C: A randomised trial. *Lancet* 2001; 358: 958-65.
- [11] Yi M, Villanueva RA, Thomas DL, Wakita T, Lemon SM. Production of infectious genotype 1a hepatitis C virus (Hutchinson strain) in cultured human hepatoma cells. *Proc Natl Acad Sci U S A* 2006; 103: 2310-5.
- [12] Sarrazin C, Zeuzem S. Resistance to direct antiviral agents in patients with hepatitis C virus infection. *Gastroenterology* 2010; 138: 447-62.
- [13] Lin C. HCV NS3-4A serine protease. In: Tan SL, Eds. Hepatitis C viruses: Genomes and molecular biology. Horizon Bioscience: Norfolk, 2006; pp. 163-206.
- [14] Lin K. Development of novel antiviral therapies for hepatitis C virus. *Virol Sin* 2010; 25: 246-66.
- [15] Cummings MD, Lindberg J, Lin T-I, et al. Induced-fit binding of the macrocyclic noncovalent inhibitor TMC435 to its HCV NS3/NS4A protease target. *Angew Chem Int Ed* 2010; 49: 1632-5.
- [16] Lemke CT, Goudreau N, Zhao S, et al. Combined X-ray, NMR, and kinetic analyses reveal uncommon binding characteristics of the hepatitis C virus NS3-NS4A protease inhibitor BI 201335. *J Biol Chem* 2011; 286: 11434-43.
- [17] Romano KP, Ali A, Royer WE, Schiffer CA. Drug resistance against HCV NS3/4A inhibitors is defined by the balance of substrate recognition versus inhibitor binding. *Proc Natl Acad Sci 2010*; 107: 20986-91.
- [18] McHutchison JG, Patel K. Future therapy of hepatitis C. *Hepatology* 2002; 36: s245-s52.
- [19] Tong L, Wengler G, Rossmann MG. Refined structure of sindbis virus core protein and comparison with other chymotrypsin-like serine proteinase structures. *J Mol Biol* 1993; 230: 228-47.
- [20] Lamarre D, Anderson PC, Bailey M, et al. An NS3 protease inhibitor with antiviral effects in humans infected with hepatitis C virus. *Nature* 2003; 426: 186-9.
- [21] Llinás-Brunet M, Bailey M, Fazal G, et al. Peptide-based inhibitors of the hepatitis C virus serine protease. *Bioorg Med Chem Lett* 1998; 8: 1713-8.
- [22] Steinkuhler C, Biasiol G, Brunetti M, et al. Product inhibition of the hepatitis C virus NS3 protease. *Biochemistry* 1998; 37: 8899-905.
- [23] Shu-Hui C, Jason L, Yvonne Y, et al. P1 and P1; optimization of 3,4-bicycloproline P2 incorporated tetrapeptidyl alpha-ketoamide based HCV protease inhibitors. *Lett Drug Des Discovery* 2005; 2: 118-23.
- [24] Urbani A, Bianchi E, Narjes F, et al. Substrate specificity of the hepatitis C virus serine protease NS3. *J Biol Chem* 1997; 272: 9204-9.
- [25] Lindenbach BD, Rice CM. Unravelling hepatitis C virus replication from genome to function. *Nature* 2005; 436: 933-8.
- [26] Yao N, Reichert P, Taremi SS, Prosise WW, Weber PC. Molecular views of viral polyprotein processing revealed by the crystal structure of the hepatitis C virus bifunctional protease–helicase. *Structure* 1999; 7: 1353-63.
- [27] Xue W, Wang M, Jin X, Liu H, Yao X. Understanding the structural and energetic basis of inhibitor and substrate bound to the full-length NS3/4A: insights from molecular dynamics simulation, binding free energy calculation and network analysis. *Mol Biosyst* 2012; 8: 2753-65.
- [28] Pan D, Xue W, Zhang W, Liu H, Yao X. Understanding the drug resistance mechanism of hepatitis C virus NS3/4A to ITMN-191 due to R155K, A156V, D168A/E mutations: A computational study. *Biochim Biophys Acta* 2012; 1820: 1526-34.
- [29] Ontoria JM, Di Marco S, Conte I, et al. The Design and Enzyme-Bound Crystal Structure of Indoline Based Peptidomimetic Inhibitors of Hepatitis C Virus NS3 Protease. *J Med Chem* 2004; 47: 6443-6.
- [30] Sheng XC, Casarez A, Cai R, et al. Discovery of GS-9256: A novel phosphinic acid derived inhibitor of the hepatitis C virus NS3/4A protease with potent clinical activity. *Bioorg Med Chem Lett* 2012; 22: 1394-6.
- [31] Zhu J, Li Y, Yu H, et al. Insight into the structural requirements of narnaprevir-type inhibitors of NS3/NS4A protease based on HQSAR and molecular field analyses. *Comb Chem High Throughput Screen* 2012; 15: 439-50.
- [32] Barbato G, Cicero DO, Cordier F, et al. Inhibitor binding induces active site stabilization of the HCV NS3 protein serine protease domain. *EMBO J* 2000; 19: 1195-206.
- [33] McCoy MA, Senior MM, Gesell JJ, Ramanathan L, Wyss DF. Solution structure and dynamics of the single-chain hepatitis C virus NS3 protease NS4A cofactor complex. *J Mol Biol* 2001; 305: 1099-110.
- [34] Franciscus A. Hepatitis C treatments in current clinical development. <http://www.hcvadvocate.org/hepatitis/hepC/HCVDrugs.html>.
- [35] Seiwert SD, Andrews SW, Jiang Y, et al. Preclinical characteristics of the hepatitis C virus NS3/4A protease inhibitor ITMN-191 (R7227). *Antimicrob Agents Chemother* 2008; 52: 4432-41.
- [36] White PW, Llinás-Brunet M, Amad M, et al. Preclinical characterization of BI 201335, a C-terminal carboxylic acid inhibitor of the hepatitis C virus NS3-NS4A protease. *Antimicrob Agents Chemother* 2010; 54: 4611-8.
- [37] Martinez A, Gish RG. Future of allopathic hepatitis C treatment. In: Tina M. St. John M. Sandt L, Eds. Hepatitis C choice. Caring Ambassadors Program, Inc., 2008; pp. 150.
- [38] Kieffer TL, Sarrazin C, Miller JS, et al. Telaprevir and pegylated interferon-alpha-2a inhibit wild-type and resistant genotype 1

- [39] hepatitis C virus replication in patients. *Hepatology* 2007; 46: 631-9.
- [40] Sarrazin C, Kieffer TL, Bartels D, et al. Dynamic hepatitis C virus genotypic and phenotypic changes in patients treated with the protease inhibitor telaprevir. *Gastroenterology* 2007; 132: 1767-77.
- [41] Tong X, Bogen S, Chase R, et al. Characterization of resistance mutations against HCV ketoamide protease inhibitors. *Antiviral Res* 2008; 77: 177-85.
- [42] Zhou Y, Bartels DJ, Hanzelka BL, et al. Phenotypic characterization of resistant Val36 variants of hepatitis C virus NS3/4A serine protease. *Antimicrob Agents Chemother* 2008; 52: 110-20.
- [43] Lagace L, White PW, Bousquet C, et al. In vitro resistance profile of the hepatitis C virus NS3 protease inhibitor BI 201335. *Antimicrob Agents Chemother* 2012; 56: 569-72.
- [44] Laohpongspaisan C, Rungrotmongkol T, Intarathep P, et al. Why amantadine loses its function in influenza m2 mutants: MD simulations. *J Chem Inf Model* 2009; 49: 847-52.
- [45] Rungrotmongkol T, Frecer V, De-Eknamkul W, Hannongbua S, Miertus S. Design of oseltamivir analogs inhibiting neuraminidase of avian influenza virus H5N1. *Antiviral Res* 2009; 82: 51-8.
- [46] Rungrotmongkol T, Udommaneethanakit T, Frecer V, Miertus S. Combinatorial design of avian influenza neuraminidase inhibitors containing pyridoline core with a reduced susceptibility to viral drug resistance. *Comb Chem High Throughput Screen* 2010; 13: 268-77.
- [47] Lee VS, Nimmanpipug P, Aruksakunwong O, et al. Structural analysis of lead fullerene-based inhibitor bound to human immunodeficiency virus type 1 protease in solution from molecular dynamics simulations. *J Mol Graph Model* 2007; 26: 558-70.
- [48] Punkvong A, Saparpakorn P, Hannongbua S, et al. Investigating the structural basis of arylamides to improve potency against *M. tuberculosis* strain through molecular dynamics simulations. *Eur J Med Chem* 2010; 45: 5585-93.
- [49] Rungrotmongkol T, Nunthaboot N, Malaisree M, et al. Molecular insight into the specific binding of ADP-ribose to the nsP3 macro domains of chikungunya and venezuelan equine encephalitis viruses: Molecular dynamics simulations and free energy calculations. *J Mol Graph Model* 2010; 29: 347-53.
- [50] Khuntawee W, Rungrotmongkol T, Hannongbua S. Molecular dynamic behavior and binding affinity of flavonoid analogues to the cyclin dependent kinase 6/cyclin D complex. *J Chem Inf Model* 2012; 52: 76-83.
- [51] da Cunha EFF, Ramalho TC, Taft CA, de Alencastro RB. Computer-assisted analysis of the interactions of macrocyclic inhibitors with wild type and mutant D168A hepatitis C virus NS3 serine protease. *Lett Drug Des Discov* 2006; 3: 17-28.
- [52] Wei HY, Lu CS, Lin TH. Exploring the P2 and P3 ligand binding features for hepatitis C virus NS3 protease using some 3D QSAR techniques. *J Mol Graph Model* 2008; 26: 1131-44.
- [53] Arasappan A, Bennett F, Bogen SL, et al. Discovery of narlaprevir (SCH 900518): A potent, second generation HCV NS3 serine protease inhibitor. *ACS Med Chem Lett* 2010; 1: 64-9.
- [54] Bogen SL, Arasappan A, Bennett F, et al. Discovery of SCH446211 (SCH6): A new ketoamide inhibitor of the HCV NS3 serine protease and HCV subgenomic RNA replication. *J Med Chem* 2006; 49: 2750-7.
- [55] Han W, Hu Z, Jiang X, Decicco CP. α -Ketoamides, α -ketoesters and α -diketones as HCV NS3 protease inhibitors. *Bioorg Med Chem Lett* 2000; 10: 711-3.
- [56] Yip Y, Victor F, Lamar J, et al. Discovery of a novel bicycloproline P2 bearing peptidyl α -ketoamide LY514962 as HCV protease inhibitor. *Bioorg Med Chem Lett* 2004; 14: 251-6.
- [57] Bogen SL, Arasappan A, Velazquez F, et al. Discovery of potent sulfonamide P4-capped ketoamide second generation inhibitors of hepatitis C virus NS3 serine protease with favorable pharmacokinetic profiles in preclinical species. *Bioorg Med Chem* 2010; 18: 1854-65.
- [58] Chen XK, Nair L, Vibulbhan B, et al. Second-generation highly potent and selective inhibitors of the hepatitis C virus NS3 serine protease. *J Med Chem* 2009; 52: 1370-9.
- [59] Nair LG, Bogen S, Ruan S, et al. Towards the second generation of boceprevir: Dithianes as an alternative P2 substituent for 2,2-dimethyl cyclopropyl proline in HCV NS3 protease inhibitors. *Bioorg Med Chem Lett* 2010; 20: 1689-92.
- [60] Nair LG, Sannigrahi M, Bogen S, et al. P4 capped amides and lactams as HCV NS3 protease inhibitors with improved potency and DMPK profile. *Bioorg Med Chem Lett* 2010; 20: 567-70.
- [61] Velázquez F, Sannigrahi M, Bennett F, et al. Cyclic sulfones as novel P3-caps for hepatitis C virus NS3/4A (HCV NS3/4A) protease inhibitors: Synthesis and evaluation of inhibitors with improved potency and pharmacokinetic profiles. *J Med Chem* 2010; 53: 3075-85.
- [62] Venkatraman S, Blackman M, Wu W, et al. Discovery of novel P3 sulfonamide-capped inhibitors of HCV NS3 protease. Inhibitors with improved cellular potencies. *Bioorg Med Chem* 2009; 17: 4486-95.
- [63] Venkatraman S, Velázquez F, Wu W, et al. Potent ketoamide inhibitors of HCV NS3 protease derived from quaternized P1 groups. *Bioorg Med Chem Lett* 2010; 20: 2151-5.
- [64] Plewczynski D, Łaziewski M, Augustyniak R, Ginalski K. Can we trust docking results? Evaluation of seven commonly used programs on PDBbind database. *J Comput Chem* 2011; 32: 742-55.
- [65] Wang R, Lu Y, Fang X, Wang S. An extensive test of 14 scoring functions using the PDBbind refined set of 800 protein-ligand complexes. *J Chem Inf Comput Sci* 2004; 44: 2114-25.
- [66] Ismail NS, El Dine RS, Hattori M, Takahashi K, Ihara M. Computer based design, synthesis and biological evaluation of novel indole derivatives as HCV NS3/4A serine protease inhibitors. *Bioorg Med Chem* 2008; 16: 7877-87.
- [67] Takaya D, Yamashita A, Kamijo K, et al. A new method for induced fit docking (GENIUS) and its application to virtual screening of novel HCV NS3/4A protease inhibitors. *Bioorg Med Chem* 2011; 19: 6892-905.
- [68] Li X, Zhang W, Qiao X, Xu X. Prediction of binding for a kind of non-peptidic HCV NS3 serine protease inhibitors from plants by molecular docking and MM-PBSA method. *Bioorg Med Chem* 2007; 15: 220-6.
- [69] Arad-Haase G, Chuartzman SG, Dagan S, et al. Mechanical unfolding of acylphosphatase studied by single-molecule force spectroscopy and MD simulations. *Biophys J* 2010; 99: 238-47.
- [70] Arsawang U, Saengsawang O, Rungrotmongkol T, et al. How do carbon nanotubes serve as carriers for gemcitabine transport in a drug delivery system? *J Mol Graphics Modell* 2011; 29: 591-6.
- [71] Mai BK, Viet MH, Li MS. Top leads for swine influenza A/H1N1 virus revealed by steered molecular dynamics approach. *J Chem Inf Model* 2010; 50: 2236-47.
- [72] Shen Z, Cheng F, Xu Y, et al. Investigation of indazole unbinding pathways in CYP2E1 by molecular dynamics simulations. *PloS One* 2012; 7: e33500.
- [73] Prongay AJ, Guo Z, Yao N, et al. Discovery of the HCV NS3/4A protease inhibitor (IR,5S)-N-[3-amino-1-(cyclobutylmethyl)-2,3-dioxopropyl]-3-[2(S)-[[[(1,1-dimethyl ethyl)amino]carbonyl]amino]-3,3-dimethyl-1-oxobutyl]-6,6-dimethyl-3-azabicyclo [3.1.0] hexan-2(S)-carboxamide (Sch 503034) II. Key steps in structure-based optimization. *J Med Chem* 2007; 50: 2310-8.
- [74] Perni RB, Chandorkar G, Cottrell KM, et al. Inhibitors of hepatitis C virus NS3/4A protease. Effect of P4 capping groups on inhibitory potency and pharmacokinetics. *Bioorg Med Chem Lett* 2007; 17: 3406-11.
- [75] Meeprasert A, Khuntawee W, Kamlungsua K, et al. Binding pattern of the long acting neuraminidase inhibitor laninamivir towards influenza A subtypes H5N1 and pandemic H1N1. *J Mol Graph Model* 2012; 38: 148-54.
- [76] Rungrotmongkol T, Udommaneethanakit T, Malaisree M, et al. How does each substituent functional group of oseltamivir lose its activity against virulent H5N1 influenza mutants? *Biophys Chem* 2009; 145: 29-36.
- [77] Sormnee P, Rungrotmongkol T, Saengsawang O, et al. Understanding the molecular properties of doxorubicin filling inside and wrapping outside single-walled carbon nanotubes. *J Comput Theor Nanos* 2011; 8: 1385-91.
- [78] Frisch MJ, Trucks GW, Schlegel HB, et al. Gaussian 03, Revision C.02. Gaussian, Inc.: Wallingford CT 2004.
- [79] Case DA, Cheatham TE, Darden T, et al. The amber biomolecular simulation programs. *J Comput Chem* 2005; 26: 1668-88.
- [80] Case DA, Darden TA, Cheatham III TE, et al. AMBER 10. University of California, San Francisco, 2008.
- [81] Duan Y, Wu C, Chowdhury S, et al. A point-charge force field for molecular mechanics simulations of proteins based on condensed-

- phase quantum mechanical calculations. *J Comput Chem* 2003; 24: 1999-2012.
- [81] Wang J, Wolf RM, Caldwell JW, Kollman PA, Case DA. Development and testing of a general amber force field. *J Comput Chem* 2004; 25: 1157-74.
- [82] Sousa da Silva AW, Vranken WF. ACPYPE - AnteChamber PYthon Parser interfacE. *BMC Res Notes* 2012; 5: 367.
- [83] Irwin JJ, Shoichet BK. ZINC - A free database of commercially available compounds for virtual screening. *J Chem Inf Model* 2004; 45: 177-82.
- [84] Korb O, Stützle T, Exner TE. Empirical scoring functions for advanced protein-ligand docking with PLANTS. *J Chem Inf Model* 2009; 49: 84-96.
- [85] Jorgensen WL, Chandrasekhar J, Madura JD, Impey RW, Klein ML. Comparison of simple potential functions for simulating liquid water. *J Chem Phys* 1983; 79: 926-35.
- [86] Hess B, Kutzner C, van der Spoel D, Lindahl E. GROMACS 4: Algorithms for highly efficient, load-balanced, and scalable molecular simulation. *J Chem Theory Comput* 2008; 4: 435-47.
- [87] Van Der Spoel D, Lindahl E, Hess B, et al. GROMACS: Fast, flexible, and free. *J Comput Chem* 2005; 26: 1701-18.
- [88] Hess B, Bekker H, Berendsen HJC, Fraaije JGEM. LINCS: A linear constraint solver for molecular simulations. *J Comput Chem* 1997; 18: 1463-72.
- [89] Darden T, York D, Pedersen L. Particle mesh ewald: An N [Center-dot] Log(N) method for ewald sums in large systems. *J Chem Phys* 1993; 98: 10089-92.
- [90] Essmann U, Perera L, Berkowitz ML, et al. A smooth particle mesh ewald method. *J Chem Phys* 1995; 103: 8577-93.
- [91] Chovancova E, Pavelka A, Benes P, et al. CAVER 3.0: A tool for the analysis of transport pathways in dynamic protein structures. *PLoS Comput Biol* 2012; 8: e1002708.
- [92] Petrek M, Otyepka M, Banas P, et al. CAVER: A new tool to explore routes from protein clefts, pockets and cavities. *BMC Bioinformatics* 2006; 7: 316.
- [93] Kumar S, Li MS. Biomolecules under mechanical force. *Physics Reports* 2010; 486: 1-74.
- [94] Carrion-Vazquez M, Li H, Lu H, et al. The mechanical stability of ubiquitin is linkage dependent. *Nat Struct Biol* 2003; 10: 738-43.
- [95] Kitchen DB, Decornez H, Furr JR, Bajorath J. Docking and scoring in virtual screening for drug discovery: Methods and applications. *Nat Rev Drug Discov* 2004; 3: 935-49.

Received: June 30, 2013

Accepted: August 27, 2013